Cutting Load Capacity of End Mills with Complex Geometry

J.A. Nemes[1], S. Asamoah-Attiah[1], and E. Budak[2]
[1]Department of Mechanical Engineering, McGill University, Montreal, Quebec, Canada
[2]Faculty of Engineering and Natural Sciences, Sabanci University, Istanbul, Turkey
Submitted by L. Kops (1), Montreal, Canada

Abstract
Cutting load capacity of cemented carbide end mills with high length-to-diameter ratios is determined from critical geometric and loading parameters, including a stress concentration factor (SCF) to account for serrated edges, which is determined by finite element analysis. Tensile strengths are characterised using a statistical Weibull analysis from 4-point bend tests of cemented carbide blanks of two different diameters. The approach is used to predict probability of survival for cutters under different loading conditions. Results are compared to measured failure cutting loads under service conditions as well as to those measured in static three point bend tests.

Keywords: Milling, Cutter, Failure

1 INTRODUCTION

Milling is widely used in industry for machining a variety of parts. Productivity and part quality improvement in milling using process modeling, monitoring and control methods have been addressed in many studies. Surface finish, tolerance integrity of the part, and chatter stability are common constraints that have to be considered in process improvement [1]. Tool breakage can also become a limitation that is particularly of importance for heavy roughing operations. When the axial depth of cut and gauge length (L) of the end mill are very large compared to the diameter (D) (say L/D of over 8) bending stresses in the tool can become extremely high causing shank breakage. Such is the case in flank milling of gas turbine engine compressors [2], which was the application considered in this study. In these cases, the material removal rate (MRR) is significantly reduced as a very small chip thickness, usually much smaller than the allowable chip load for the given cutting edge, is used to keep the cutting forces low. Predicting the breakage limit of end mills with complex geometry such as taper ball end mills can be effective in eliminating overloading and may also be used in process optimization by analyzing the effect of various geometric details on the stress, and thus increasing MRR. Tool breakage investigations have mainly focused on edge chipping and breakage detection. Determination of the stresses in milling cutters with complex geometry is not straightforward due to the complicated geometry these cutters can have. Taper ball end mills have varying diameter, helix angle and flute depth in the axial direction. Serrations that are used on the roughing cutters to reduce forces, increase stability and improve chip breakage further complicate the geometry.

Assessment of tool breakage requires not only knowledge of the state of stress but also a criteria for evaluation of fracture. Point fracture criteria appropriate for brittle materials, including maximum stress and maximum strain criteria, are discussed by Tagaki and Shaw [3]. Regardless of the criteria used, however, point criteria, by themselves, cannot describe the variability of measured strengths in brittle materials. An alternative to point failure criteria is the use of fracture mechanics, where strength variability can be attributed to the variation of flaw shapes and sizes in the material. Linear elastic fracture mechanics methods are appropriate, such that for a given crack size and applied stress, the stress intensity factor, K_I, can be determined. K_I, has been tabulated for many different geometries or it can be found from the change in compliance as was done by Shibasaka, et. al [4]. The fracture toughness is compared to a critical fracture toughness, K_{IC}, which must be determined from testing. For ceramic materials, the critical fracture toughness can be found using microhardness tests, either directly [5] or by using bend tests of specimens in which the flaw was created using an indenter [4]. Growth of cracks during fatigue loading can also be considered using fracture mechanics by determining a ΔK_I for the loading cycle and determining the crack growth law, da/dN, from which tool life could be estimated. However, because of the low fracture toughness of many tool materials critical crack lengths are correspondingly small. For example, K_{IC} has been determined to be 13 MPa $m^{1/2}$ for a WC ceramic [5], which results in a critical flaw size of < 0.1 mm at stresses comparable to the tensile strength. Such small critical crack sizes make their detection and/or monitoring extremely challenging.

Determination of tool stresses from known cutting forces has been accomplished using both analytical expressions [6] and finite element methods [7-10]. Although finite element analysis has been demonstrated to provide reliable determination of stresses, the complex 3D geometry of the tapered mill cutter makes their modeling very time consuming, particularly when a wide variety of cutter geometries is employed as in a large manufacturing organization. Thus a more robust approach is desired.

2 STRESSES IN THE CUTTER

2.1 Milling Forces

Several cutting force models used in the analysis of the milling process are discussed by Budak [2]. In this study, however, the focus is to determine the maximum load capacity of an end mill and therefore milling forces are assumed to be known. The force is taken to be uniform along the length, which is an acceptable assumption for cases where the maximum stress is above the cutting depth.

2.2 Stress Analysis

The tapered mill cutter is idealized as a cantilever beam of varying cross-section, defined by an equivalent radius, using an approach similar to that by Kops and Vo [11] for determining end mill deflection. The analysis is based on Euler-Bernoulli beam theory, with normal stresses much greater than shear stress, such that the normal stress is the principal stress. The idealized cutter geometry is shown in Figure 1, where R_b is the ball radius of cutter, W is the distributed load, ϕ is the taper angle, R_s is the shank radius, d is the cutting depth, H is the flute length, L is the length of cutter, and fd is the flute depth.

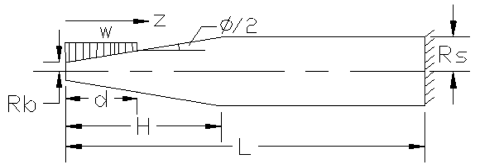

Figure 1: Loading conditions of the cutters.

The cross sections along the tapered length of the 3-flute and the 4-flute cutters are as shown in Figure 2.

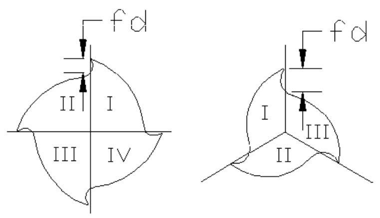

Figure 2: Cross section of the 4-flute and 3-flute cutters.

To ease computation of the total moment of inertia, the cross sections were divided into regions depicted in Figure 2. Each region is bounded by an arc of radius *r* and center (*x*, *y*), and the lines shown. It is obvious that by computing the inertia matrix of one region the other regions can be obtained by appropriate transformation. From Figure 3 using the cosine law we can define an equivalent radius R_{eq} for region *I* in terms of *r* and the position vector of the center of the arc respect to the *x*- and *y*-axes as

$$R_{eq}(\theta)_{3-Flutes} = p\cos(\theta + \pi/3) + f(\theta)$$
$$R_{eq}(\theta)_{4-Flutes} = p\sin(\theta) + g(\theta) \qquad (1)$$

where

$$f(\theta) = \sqrt{p^2\cos^2(\theta + \pi/3) + (r^2 - p^2)}$$
$$g(\theta) = \sqrt{p^2\sin^2(\theta) + (r^2 - p^2)}$$

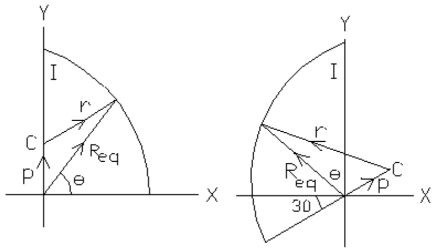

Figure 3: (a) Region I of a 4-flute cutter; (b) Region I of a 3-flute cutter.

Note that Eq. (1) defines the equivalent radius at the end of the flute length . From the flute depth and the shank radius the minimum equivalent radius along the taper length is computed. Now using similar triangles the equivalent radius can be expressed in terms of the distance z along the flute length of the cutters as

$$R(z,\theta) = R_{eq}(\theta) + (z - H)\tan\phi \qquad (2)$$

Knowing R(z,θ) the moment of inertia M_{xx}, M_{yy} and M_{xy} can be obtained as

$$M_{xx}(z) = \int_A \rho^3 \sin^2\theta \, d\rho \, d\theta$$
$$M_{yy}(z) = \int_A \rho^3 \cos^2\theta \, d\rho \, d\theta \qquad (3)$$
$$M_{xy}(z) = \int_A \rho^3 \sin\theta \cos\theta \, d\rho \, d\theta$$

where $0 \geq \rho < R(z,\theta)$ and $0 \geq \theta < \pi/2$ for 4-flute cutters and $0 \geq \theta < 2\pi/3$ for 3-flute cutters. To account for the presence of the serrations on the cutter, finite element analysis is used to determine stress concentration factors. Several serration patterns were considered with the SCF ranging from 2.04 to 2.21. Knowing the stress concentration and the geometric parameters shown in Fig. 1, the maximum stress along the length of the cutter can be determined for a given cutting depth and distributed loading intensity. Figure 4 shows the computed stress at the outside radius for a 4-flute cutter for three different cutting depths, with the same total load of 10.4 kN.

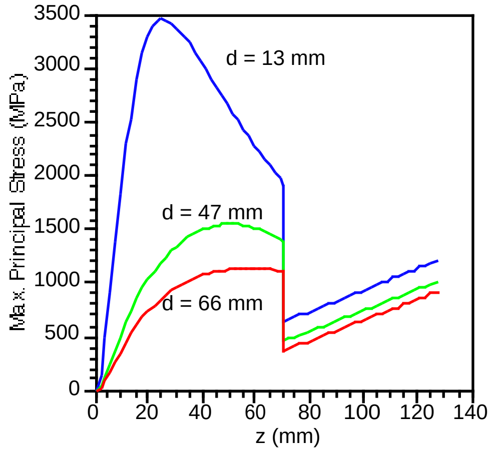

Figure 4: Variation of stress along the length of the cutter for three cutting depths.

3 STRENGTH OF CEMENTED CARBIDE MATERIAL

3.1 Blank Tests

To determine the tensile strength of the carbide material, equal span 4 pt. bend tests with a total span of 254 mm were performed on circular cemented carbide blanks with diameters of 12.5 mm (B12) and 25.4 mm (B25). The blanks were WC-6% Co, with a minimum Rockwell Hardness A of 92.8. Ten blanks of each size were tested. For the 12.5 mm diameter specimens the mean failure stress was 2131 MPa with a standard deviation of 503 MPa and for the 25 mm specimens the mean failure stress and standard deviation were 1262 MPa and 214 MPa, respectively.

3.2 Weibull analysis

Although there are a number of probablistic theories, that proposed by Weibull is universally recognized. The theory has been described as the 'weak-link' model since it is the largest flaw within the volume that will determine breaking strength. As a result, the stress distribution over the entire volume is considered and the strength of the material decreases as volume increases. For an infinitesimal volume the risk of rupture, R, depends only on stress. Weibull postulated that for a unit volume

$$R=\left(\frac{\sigma-\sigma_u}{\sigma_0}\right)^m \tag{4}$$

where σ is the applied stress, σ_u is the stress below which there is zero probability of failure, σ_0 is a characteristic strength analogous to the mean strength, and m is the Weibull modulus, which characterizes material variability. The Weibull parameters for a unit volume can be determined from Eq. (4) and the results of the 4 pt. bend tests, by plotting the double logarithm of the probability of survival, S (V_0), defined as exp (-R) vs. the log of the failure stress. The results are shown in Figure 5 for the two blank diameters. To compare results or to use the results to evaluate the strength of cutters, the stress distribution over the volume must be considered. Thus the probability of survival is S(V) is determined as

$$S(V)=\exp\left(-\int_V\left(\frac{\sigma}{\sigma_0}\right)^m dV\right) \tag{5}$$

The tensile stress distribution in the 4 pt. bend test is

$$\sigma(r,\theta,z)=\sigma_{\max}\left(\frac{r}{a}\right)\left(\frac{3z}{L}\right)\cos\theta \qquad 0\le z\le\frac{L}{3}$$

$$\sigma(r,\theta,z)=\sigma_{\max}\left(\frac{r}{a}\right)\cos\theta \qquad \frac{L}{3}\le z\le\frac{2L}{3} \tag{6}$$

for $0 \le r \le a$ and $-\pi/2 \le \theta \le \pi/2$. For an equal probability of survival, evaluating (6) for the two size blanks gives the relationship

$$\frac{(\sigma_{\max})_1}{(\sigma_{\max})_2}=\left(\frac{a_2}{a_1}\right)^{2/m} \tag{7}$$

For a Weibull modulus of 5, the stress ratio for an equal probability of survival for the two size blanks would be 1.32, which explains to some degree the difference in mean stress observed for the two size blanks. However, differences in processing may also be a factor.

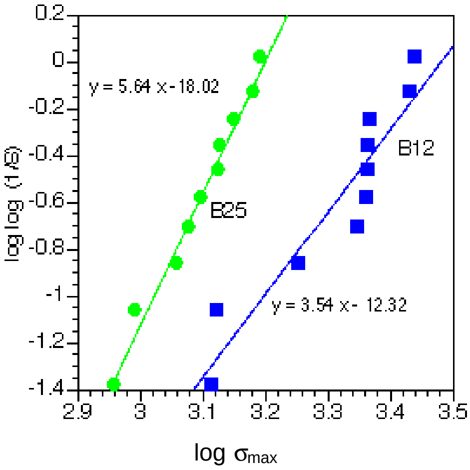

Figure 5: Determination of Weibull parameters from blank tests.

4 APPLICATION TO MILL CUTTERS

4.1 Probability of Survival

To test the proposed stress analysis and failure model, tapered mill cutters were tested to failure under both 3-pt static bend testing as well as during cutting conditions, where loads were recorded using a spindle-mounted dynamometer. To determine the probability of survival the stress distribution must be integrated over the volume. The variation of stress shown in Figure 4, is used for the longitudinal distribution where the circumferential variation of stress in the cutters in three-point bend is the same as that for the blanks. The stress distibution is integrated numerically. It is then possible to determine the max stress in the cutter, $(\sigma_{max})_{c3}$ that has an equal probability of survival as a blank in 4 pt. bend with maximum stress $(\sigma_{max})_B$.

$$(\sigma_{\max})_{c3}=(\sigma_{\max})_B\left[.00328\frac{(m+3)}{(m+1)(m+2)}L_B a_B^2\right]^{1/m} \tag{8}$$

where L_B and a_B are in mm. Using the Weibull parameters derived from the 25.4 mm blanks, the above expression reduces to

$$(\sigma_{\max})_{c3}=1.73(\sigma_{\max})_B \tag{9}$$

Due to rotation, the stress distribution of cutters in service is independent of θ, thus a much greater volume of material is subjected to tensile stress. As a result, for a cutter in service the maximum stress, $(\sigma_{max})_{cs}$ with an equal probability of survival as that of a cutter in 3-pt bend, $(\sigma_{max})_{c3}$ is

$$(\sigma_{\max})_{cs}=.724(\sigma_{\max})_{c3} \tag{10}$$

Using (9) and (10) the maximum stress for a cutter of arbitrary size in service having an equal probability of survival as the 25 mm blank under 4 pt bend is

$$(\sigma_{\max})_{cs}=1.25\left(\frac{87.63}{H}\right)^{1/m}\left(\frac{9.53}{R_s}\right)^{2/m}(\sigma_{\max})_B \tag{11}$$

where H and R_s are in mm. Clearly caution should be used in extrapolating to cutters of sizes considerably different than those considered here.

SPEC.	Flutes	R_b (mm)	ϕ (deg.)	R_s (mm)	H (mm)	L (mm)	σ_{max} (MPa)	S (%)
C3-00	3	3.18	8	9.53	87.6	206	1517	96.3
C3-01	3	3.18	8	9.53	87.6	210	1586	95.3
C3-02	3	3.18	8	9.53	79.8	210	1559	96.1
C3-03	3	3.18	8	9.53	95.0	224	1117	99.3
C3-04	4	5.59	7	9.53	74.9	184	3034	19.8
C3-05	4	5.59	4	9.53	100.	214	786	99.8
C3-06	4	5.59	4	9.53	100.	230	1310	98.1
C3-07	4	5.59	4	9.53	74.9	190	1683	94.4
C3-08	4	5.59	7	9.53	65.0	195	3469	4.93
C3-09	4	5.59	4	9.53	100.	227	1897	86.0

Table 1: Results of cutter 3 pt. bend tests

SPEC.	Flutes	R_b (mm)	ϕ (deg.)	R_s (mm)	H (mm)	L (mm)	W (N/mm)	d (mm)	σ_{max} (MPa)	S (%)
CS-00	4	6.35	6	9.53	66.7	102	537	12.7	2551	3.25
CS-01	4	6.35	6	9.53	66.7	95	137	47.0	1517	83.6
CS-02	4	6.35	6	9.53	66.7	95	150	66.0	1759	66.0
CS-03	4	5.59	9	11.1	71.0	127	627	12.7	2482	1.45
CS-04	4	5.59	9	11.1	71.0	127	261	47.0	1862	43.7
CS-05	4	5.59	9	11.1	71.0	127	93	66.0	655	99.7
CS-06	4	4.6	8	9.53	75.2	102	233	12.7	3172	<.01
CS-07	4	4.6	8	9.53	75.2	102	57	47.0	1034	97.7
CS-08	4	4.6	8	9.53	75.2	102	84	66.0	1517	81.7
CS-09	3	3.18	8	7.94	70.6	170	157	12.7	1172	97.0
CS-10	3	3.18	8	7.94	70.6	170	96	47.0	1174	96.9
CS-11	3	3.18	8	7.94	70.6	170	45	66.0	586	99.9
CS-12	3	3.18	10	7.94	50.2	173	137	12.7	538	99.9
CS-13	3	3.18	10	7.94	50.2	170	150	66.0	1449	93.0

Table 2: Results of tests on cutters in service

5 RESULTS AND CONCLUSION

The calculated stress and resulting probability of survival are shown in Tables 1 and 2 for cutters in bend testing and in service. In bend testing, the mean failure stress and standard deviation are 1796 MPa and 833 MPa, respectively and in service they are 1533 MPa and 782 MPa. Comparing these results, the mean stress for cutters in service is .85 times that in 3 pt. bend, which is consistent with the result predicted by Eq. (10). The standard deviation for the two are similar, but both are higher than that for either the B12 or B25 blanks, which may be expected to the greater probability of flaws in cutters. The mean failure stress for the cutters in service is 1.21 times that of the B25 blanks, which is remarkably close to that predicted by Eq. (11). Somewhat less satisfying is the number of cutters having either a very high or very low probability of survival, which is related to the large observed standard deviation. A practical remedy for which is to use a somewhat smaller value of the Weibull parameter, m, than that used in the analysis. The method can then be used to determine the probability of survival for a cutter subjected to given loads.

6 ACKNOWLEDGMENTS

The authors would like to acknowledge the support of Pratt & Whitney Canada, particularly Mr. Don Macintosh and the assistance of Mr. Yannick Jolin.

7 REFERENCES

[1] Enache, S., Strajescu, I, Tanase, C., 1992, Determination of Tool Cutting Capacity, Annals of the CIRP, 41/1:145:149.

[2] Budak, E., 2000, Improving Part Quality in Milling of Titanium Based Impellers by Chatter Suppression and Force Control, Annals of the CIRP, 49/1:31-38.

[3] Takagi, J., Shaw, M, 1981, Evaluation of Fracture Strength of Brittle Tools, Annals of the CIRP, 30/1:53-57.

[4] Shibasaka, T., Hasimoto, H., Ueda, K., Iwata, K., 1983, Analysis of Brittle Failure of Cutting Tools Based on Fracture Mechanics, Annals of the CIRP, 32/1:37:41.

[5] Lawn, B., Marshall, D., 1979, Hardness, Toughness, and Brittleness: An Indentation Analysis, J. Amer. Ceramic Soc., 62:347:350.

[6] Chandrasekaran, H., Reddy, T., 1982, On the Nature of Cyclic Stresses in the Tool Tip in Peripheral Milling and Their Implications on Tool Fracture, Annals of the CIRP, 31/1:85-89.

[7] Chandrasekaran, H., Thuvander, A, Wisell, H., 1988, Modelling of Tool Stresses in Peripheral Milling, Annals of the CIRP, 37/1:41-44.

[8] Vichev, S., Kirov, V., Hristov, D., 1994, Strength Calculation of Cutting Tools, Int. J. Mach. Tools Manufact., 34:13-18.

[9] Kanazawa, K., Naroka, S., Igaya, N., 1997, Analytical Prediction of Failure in Cemented Carbide End-mill – Application to Several Cutting Conditions and Helix Angle 0, J. Jpn. Soc. Prec. Eng., 63:1741-1746.

[10] Kanazawa, K., Naroka, S., 1998, Analytical Prediction of Failure in Cemented Carbide End-mill – Influence of Cutting Condition and End-mill Shape, J. Jpn. Soc. Prec. Eng., 64:131-136.

[11] Kops, L., Vo, D., 1990, Determination of the Equivalent Diameter of an End Mill Based on its Compliance, Annals of the CIRP, 39/1:93-96.